Vol. 2, No. 1, pp. 23-27, June 2003

INTERNATIONAL JOURNAL OF SAFETY
www.kiis.or.kr

Numerical and Experimental Evaluation of Tensile Failure in Continuous Fiber Reinforced Ceramic Composite

Oh Heon Kwon*, Keyoung Dong Park[1] and Katsuhiko Watanabe[2]

*Department of Safety Engineering, Pukyong National University, Busan 608-739, Korea
[1]School of mechanical Engineering, Pukyong National University, Busan 608-739, Korea
[2]Institute of Industrial Science, University of Tokyo, Tokyo 153-8505, Japan

(Received April 7, 2003; Accepted June 7, 2003)

Abstract : Recently, continuous fiber reinforced ceramic composite(CFCC) has attracted attention to a number of engineers because of its significant benefit for several industrial area. This work was conducted to provide a basic characteristic of CFCC for tensile loading condition. The numerical analysis by general purpose finite element program was accomplished and compared with an experimental tensile test. The stress strain curves were expressed well by the numerical analysis and the first matrix cracking stress was in accordance with that of the experimental result. Moreover, fracture pattern was shown by kill command graphically.

Key words : tensile failure, CFCC(Continuous Fiber Ceramic Composite), matrix cracking stress, fiber bridging effect

1. Introduction

In the past two decades, a great deal of work has been devoted to the development of the advanced composite materials because of their excellent mechanical properties [1~3]. Especially, the continuous fiber reinforced ceramic composites(CFCCs) are materials which have essentially a continuous length fiber or yarn, and a matrix that converts the fiber architecture into a rigid body to protect from environment. Because fibers are significantly stronger than matrix materials, we would think that they would be stronger than monolithic ceramics of similar composite. Owing to their notable benefits, they have been used in the numerous engineering area of aerospace, hot gas filters, turbine, engine etc. As the applied load is monotonically increased, more matrix damages will develop. The matrix damages become critical point at certain load level, and accompanied by fiber fractures which may occur at any point where the local fiber strength is exceeded by applied stress. A number of investigations have studied for CFCCs [5~6]. Marshall and Cox [7] have established relations between the composite stress in tensile factor in front of a matrix crack bridged by fibers and composite strength. Curtin [8] simplified linear stress distribution in the fiber and matrix it was used where some important material behavior was excluded. Xu [9] explained the relations between ultimate strength, matrix cracking stress, fiber volume fraction and pre-exist flaw size of the composite materials. However, there are still major problems that need to be reported for a clear understanding of these CFCCs.

In the present work, a finite element analysis is carried out for a tensile loading type and transition of the fracture patterns is described according to the increasing loading. And then the relationship of matrix cracking stress and fracture pattern is shown. Futhermore the stress analysis results are compared with an experimental result.

2. Matrix cracking stress theory

The phenomenon of matrix micro cracking is an extremely important feature of CFCC. Matrix microcracking occurs when the failure strain of the matrix is lower than that of the fibers. Ignoring effects due to materials mismatch, the matrix cracking is calculated from the simple rule of mixture [10] which assumes

*Corresponding author: kwon@pknu.ac.kr

strains in fibers ε_f and matrix ε_m,

$$\sigma_c = \sigma_f v_f + \sigma_m v_m \quad (1)$$

where σ_c, σ_f, σ_m, v_f and v_m are stresses and volume fractions in composite, fiber and matrix. Now,

$$\varepsilon_m = \frac{\sigma_m}{E_m} = \varepsilon_f = \frac{\sigma_f}{E_f} \quad (2)$$

$$\text{Therefore, } \sigma'_c = (\sigma_m)_u\left[1 + V_f\left(\frac{E_f}{E_m} - 1\right)\right] \quad (3)$$

where $(\sigma_m)_u$ is the strength of the matrix and σ'_c is the stress in the composite at which matrix cracking should occur.

3. Tensile test

The used material was a commercial material comprised of unidirectional SCS6 fibre reinforced a Si_3N_4 matrix. The fiber diameter and their distribution were examined on the sample cross section normal to the fibers. Fiber distributions were uniform as shown in Figure 1. The major diameter of fiber was 177.52 μm including a 1.76 μm thick carbon rich surface coating and 49.3 μm diameter carbon core. The fiber volume fraction was estimated as 10.5% by calculating areas of fibers section in the specimen with known cross sectional area connecting fiber section center points. The volume fraction of matrix was calculated as 70.7%. The volume fraction of porosity is 18.8%.

Test specimens having straight-sided flat and reduced gage sections (i.e., dogbone) were prepared for tensile tests per ASTM C1275. The tensile test specimen configuration is shown in Figure 2. End tabs adhered to the gripped section of the test specimen were used to protect the test specimens from being damaged from the closure of the hydraulically-actuated wedge grips.

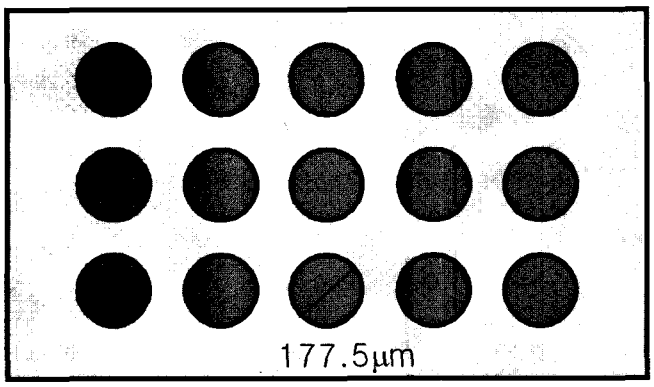

Fig. 1. A schematic of uniform fiber distribution in the specimen cross section area.

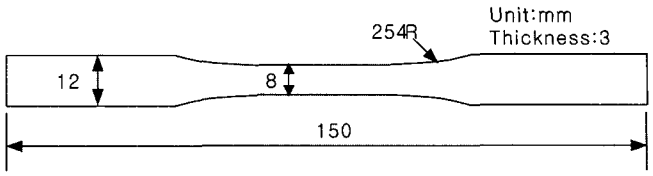

Fig. 2. The specimen configuration of the tensile test for CFCCs.

Clamping without using end tabs can produce localized damage due to the contact of the grip surface with the specimen [11]. The end tabs were made of E-glass fiber/epoxy matrix composites.

Test specimens were loaded using interchangeable, hydraulically actuated specimen grip system which could maintain an adjustable grip force without backlash and was independently activated. Gage section displacements for calculation of strain were measured using an dual extensionmeter attached by spring force to the test specimen. For the dual extensionmeter, Axis A and Axis B were on opposite faces of the gage section of the test specimen with 25 mm initial gage lengths and ranges of upper and lower strain ranges over these guage lengths of +5% to 2%, respectively. Strain was measured directly using a conventional, adhesively bonded electrical resistance strain gages.

Alignment was verified by measuring the strain on the four faces of only a strain gages dummy (steel) test specimen. The purpose of the verification procedure was to minimize the introduction of bending moments into the specimen during tensile test. The percent bending moment was calculated from the strain gage readings For four strain gages spaced 90° apart around the circumference of the gage section, percent bending moment is calculated such that

$$\%\ \text{bending moment} = \frac{[(\Delta\varepsilon_{1,3})^2 + (\Delta\varepsilon_{2,4})^2 + (\Delta\varepsilon_{1,3})^2]^{1/2}}{\varepsilon_0} \times 100 \quad (4)$$

where

$$\Delta\varepsilon_{1,3} = \frac{(\varepsilon_1 - \varepsilon_0) - (\varepsilon_3 - \varepsilon_0)}{2} = \frac{\varepsilon_1 - \varepsilon_3}{2}$$

$$\Delta\varepsilon_{2,4} = \frac{(\varepsilon_2 - \varepsilon_0) - (\varepsilon_4 - \varepsilon_0)}{2} = \frac{\varepsilon_2 - \varepsilon_4}{2}$$

$$\varepsilon_0 = \frac{(\varepsilon_1 + \varepsilon_2 + \varepsilon_3 + \varepsilon_4)}{4} \quad (5)$$

and ε_1, ε_2, ε_3 and ε_4 are the strain gage readings in units of strain. In this study, %bending was less 5% bending at an average strain of 500 μm/m in the align-

ment specimen. For displacement control, test rates of 0.1 mm/s were used.

4. Numerical approach

Numerical modeling in this study was carried out using ANSYS 6.3 code assuming tensile test. The element type was an 8-noded quadrilateral element. Elements have double mesh [12] representing fiber mesh and matrix mesh. This doesn't generate extra counterpart nodes owing to double meshes. Therefore when any load applied to any node of the mesh, it affects same both node of fibers and matrix. Figure 3 shows the concept of the double mesh element in tensile loading case.

A nonlinear incremental analysis with displacement controlled loading was carried out about tensile loading type. Accomplished total displacement was 0.5mm in tensile loading type model. At each step, conditional criteria that was based at the maximum principal stress was evaluated to fail elements, which disappear as a fracture in satisfying the failure criteria. The element disappearance means that a particular elements's stiffness reduces to near zero. The element birth and death command in ANSYS code was used to kill an element after satisfying the failure criteria. For the matrix elements, when a principle stress has greater value than ultimate strength, the matrix element would be killed as reducing the stiffness to near zero. Then, the load is transferred to the fiber element. Now, the fiber element reaches the critical stress, the element is killed. This procedure is repeated checking the stresses at the end of each load displacement step for the criteria until all steps are completed.

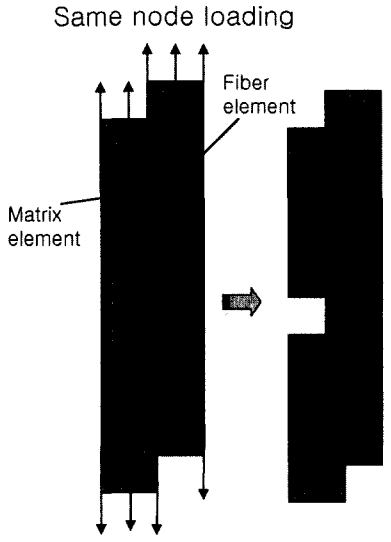

Fig. 3. An Implementation of the double meshes.

Table 1. Assumed material properties

Constituent	Volume fraction(%)	Elastic Modulus, E(GPa)	Ultimate Tensile Strength,Su(MPa)
SCS6 fiber	10.5	400	4200
matrix	70.7	150	150

The total numbers of elements and nodes were 20693 and 13360, respectively in tensile loading type specimen model. Assumed material properties used in the analysis are shown in Table 1.

The finite element model was assumed as a tensile test specimen shown in Figure 2.

5. Results and discuss

Figure 4 shows the stress strain curve for a tensile loading using double mesh finite element model.

The closed triangle symbol means matrix curve and square means fiber element. The matrix element stress is higher than fiber element stress because of low volume fraction. A matrix and fiber element stresses increase up to ultimate matrix strength linearly. The matrix element just initiates to break when the stress reaches the critical stress. But the fiber elements are keeping the healthy condition and are elongated by loading which has transferred from the matrix part. The stress strain curve of the composite shown in Figure 4 was obtained by a finite element analysis. This is near same result with that calculated by equation (3). In this study, the curve increases linearly from 0 to 53 MPa. This represents that the first matrix cracking stress for

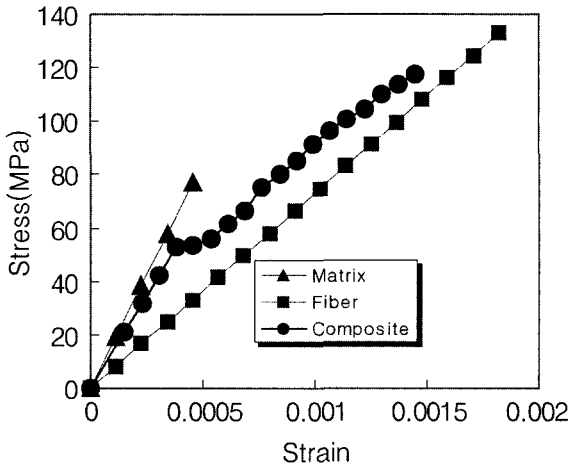

Fig. 4. The simulation stress-strain curves for each material type.

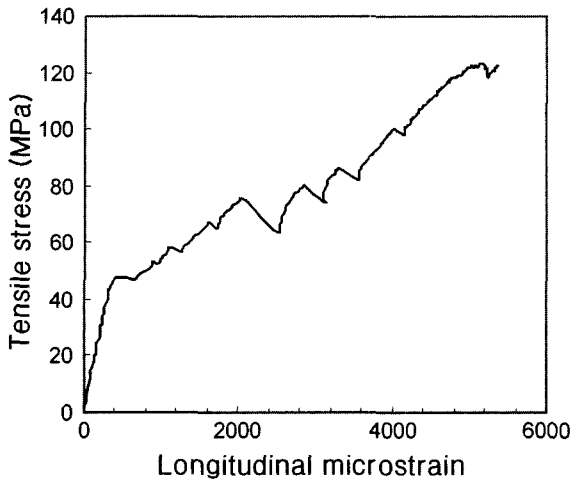

Fig. 5. Typical monotonic stress-strain curve for SCS6/Si_3N_4 CFCC.

tensile loading type is 53 MPa. After the first matrix cracking, the stress strain curve increases according to the slope of fiber element. Figure 5 shows an engineering stress strain curve from a tensile experiment. In Figure 5, the stress strain curve was also linear up to the proportional limit stress that is 50.7 MPa similar to Figure 4. However the stress increased going up and down repeatedly over a proportional limit stress against a smooth linearity of the stress strain curve from finite element analysis. This change in response shows that the proportional limit stress is the onset of nonlinearity and represents the stress at matrix cracking and which indicates the cumulative damage process area. The area beyond the point of first matrix cracking is conservatively considered the strain overload region.

These nonlinear behavior is attributed to the fiber bridging, interfacial debonding and entire matrix cracking phenomena until the fiber breaks. At the least, the presence of fiber bridging capability may help insure

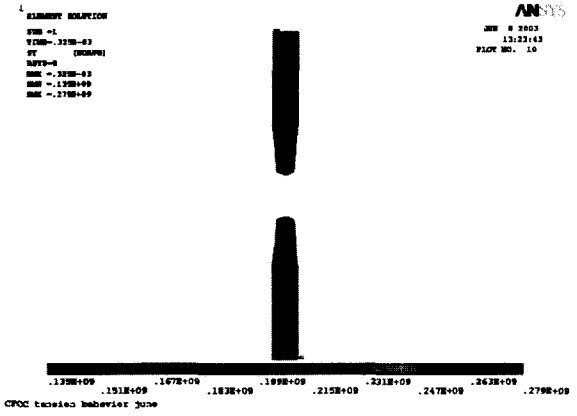

Fig. 6. The fracture pattern of the killed matrix elements at 5th load steps.

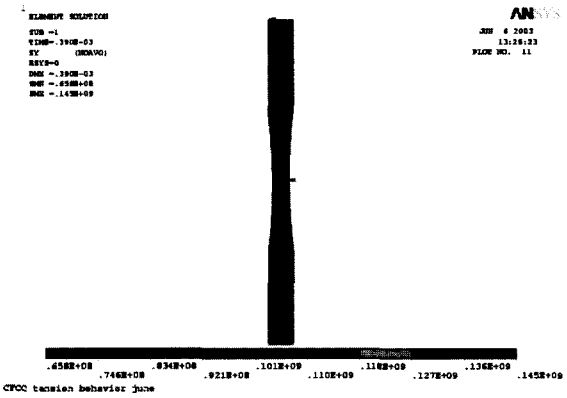

Fig. 7. The stress distribution and fiber bridging effect for fiber elements at 5th load steps.

design acceptability merely by permitting lower safety factors which catastrophic brittle failure can be avoided. Figure 6 shows a result of fracture pattern at a first matrix cracking for tensile loading model. Because neither the fiber nor matrix stresses exceed critical stress in the proportional region over 1st load step, no killed elements were not shown in a model. However, the matrix elements which exceed critical stress were killed at matrix cracking of 5th load steps. A lot of matrix elements around center region of the finite element model were killed simultaneously. Therefore, a brittle fracture pattern transversing the model occurs in the tensile loading model. Although the matrix elements were killed after an initiation of the first matrix cracking, the fiber elements exit still as unbroken situation as shown in Figure 7. And then, the load is transferred to the fiber elements that would be burdened with all of load. The fiber elements were playing a role of bridging until fibers were killed at the ultimate strength. As shown in Figures 6, 7, the matrix bridged by fibers was observed well. This fiber bridging phenomena effects the toughness of CFCC composite. Then the failure of composite can avoid catastrophic situation.

5. Conclusions

A tensile test and a FEM code ANSYS for the analysis of CFCCs behavior are described. Based on the results shown, the following conclusions can be drawn:

1) A proportional limit and a first matrix cracking stress of FEA are in accordance with those of the experimental tensile test.

2) A CFCCs can be a useful material because of ability of uncatastrophic failure owing to fiber bridging effects.

3) The first matrix cracking stresses for tensile load-

ing type are 58 MPa and 50.7 MPa for a FEA model and an experiment, respectively.

4) A stress strain curves obtained by using double element method in FEA model represented behaviors of the fiber and matrix element and the composite, respectively, well.

References

[1] O. I .Benevolenski, J. Karger-Kocsis, T. Czigany and G.Romhany, Mode I fracture resistance of glass fiber mat-reinforced polypropylene composites at various degree of consolidation, Composites, Part A, Vol. 80, in press, 2003.

[2] M. G. Jenkins, J. P. Piccola, Jr. and E. Lara-Curzio, Fracture Mechanics of Ceramics, Vol. 12, pp. 267~282, 1996.

[3] R. T. Bhatt, Ceramic International, Tensile Properties and Micro structural Characterization of Hi-Nicalon SiC/RBSN Composites, Vol. 26, pp. 535~539, 2000.

[4] K. Liao and K. Reifsnider, A tensile Strength model for Unidirectional fiber-reinforced brittle Matrix composites, Int. Jour. of Fracture, Vol. 106, pp. 95~115, 2000.

[5] S. K. Mital, Computational simulation of continuous fiber reinforced ceramic matrix composites behavior, Journal of advanced materials, Vol. 32, No. 1, pp. 46~59, 2000.

[6] A. G. Evans and D. B. Marshall, Mechanical Behavior of Ceramic matrix Composites, Fiber Reinforced Ceramic Composite Materials, Processing and Technology, Edited by General Atomics, San Diego, pp. 8~10, 1990.

[7] D. B. Marshall, B. N. Cox and A.G.Evans, The mechanics of matrix cracking in brittle matrix fiber composites, Acta Metallurgica, Vol. 33, pp. 2013~2021, 1985.

[8] W. A. Curtin, Ultimate strength of fiber reinforced ceramics and metals, Composite A, Vol. 24, pp. 98~103, 1993.

[9] H. H. K. Xu, P. Ostertag and L. M. Braun, Short-Crack mechanical Properitiesand failure Mechanism of Si3N4 matrix/SiC fiber Composite, J. Am. Ceram. Soc., Vol. 77, pp. 1889~1896, 1994.

[10] D. C. Phillips, Long-fiber reinforced ceramics, pp. 190~194, Ceramic-Matrix Composite, Blackie, 1992.

[11] C. X. Campbell, MS Thesis, University of Washington, Seattle, 1998.

[12] K. Y. Mark, MS Thesis, University of Washington, 1996.